

Early expression of the *tbx22* gene in zebrafish influences positioning of pharyngeal arch cartilages

Tammy Lynne Silva¹, Angela Allard Cox¹, Vijay Padhmanaban Boominathan², Peter Alan Jezewski³, Tracie Lee Ferreira²

¹Department of Biology, University of Massachusetts Dartmouth, Dartmouth, USA

²Department of Bioengineering, University of Massachusetts Dartmouth, Dartmouth, USA

³Department of Periodontology, Institute of Oral Health Research, University of Alabama at Birmingham, Birmingham, USA

Email: tferreira@umasds.edu

Received 17 August 2012; revised 20 September 2012; accepted 28 September 2012

ABSTRACT

Mutations in human *tbx22* cause X-linked cleft palate with ankyloglossia syndrome. The two zebrafish *tbx22* splice isoforms, *tbx22-1* and *tbx22-2*, encode proteins of 444 and 400 amino acids, respectively. Zebrafish *tbx22* mRNA expression mirrors mammalian *tbx22* expression and is consistent with early patterning of the vertebrate face. In zebrafish, *tbx22* mRNA is strongly expressed during early pharyngeal arch development in the ventral mesenchyme, and a later expression domain is found in ectomesenchymal cells underlying the stomodeum, a bilaminar epithelial structure demarcating the early forming mouth. Therefore, *tbx22* is hypothesized to be involved in craniofacial development. The objective of this work is to characterize the role of *tbx22* during craniofacial development in zebrafish. *tbx22* knockdown revealed that defects in *tbx22* signaling cause mild clefting, joint defects and dorsoventral patterning defects in cartilages. Quantitative PCR and *in situ* analysis revealed that knockdown of *tbx22* also causes a dramatic decrease in expression of *osr1* and *gdf5*. Craniofacial patterning is dependent on proper signals from endoderm, mesoderm and ectoderm. The early influence of *tbx22* on signals within the ventral mesenchyme impacts the domains of several key pharyngeal arch signals, thereby helping to regulate proper patterning of the developing jaw.

Keywords: Zebrafish; *tbx* Signaling; Pharyngeal Pouch

1. INTRODUCTION

Craniofacial development relies on signals emanating from the endoderm, ectoderm and the brain. Proper formation and positioning of craniofacial cartilages is driven by numerous secreted signals in each of these three cell layers. As the Cranial Neural Crest (CNC) cells migrate

ventrally from the dorsal neural tube they are influenced by signals such as sonic hedgehog produced by the foregut endoderm [1], forebrain expression of FGF-R [2], and Bone Morphogenetic Protein (BMP) and Noggin influence skeletal formation [3,4]. Within each pharyngeal arch there are dorsal and ventral components which are specified by additional signals such as those found in the endothelin (edn) pathway [3]. The regulation of these secreted signals is accomplished through a variety of transcription factors including members of the MSX, DLX, *OSR* and *tbx* families [5-8]. It is therefore critical that in addition to understanding how secreted ligands and receptors regulate craniofacial development, that we also unravel the regulation of their transcription.

The *T-box* genes are an ancient family of transcription factors that are well conserved throughout all metazoans [9,10]. All *T-box* genes share a conserved homology domain that encodes a polypeptide region known as the *T-box* [9]. The *T-box* region of the protein possesses DNA binding activity and binds to a specific sequence of DNA called the T-site [9,11]. *T-box* proteins are thought to be important regulators of early mesoderm induction, specification, movement, patterning, as well as somite formation [10,11]. *T-box* genes are usually expressed in highly specific patterns and *tbx* genes expressed in the same area can function additively or antagonistically to directly regulate genes that control patterning and differentiation of cell types in the region where they are expressed [9-11].

Characterization of several *tbx* genes suggests a role for these genes in craniofacial development [12-14]. *tbx22* is a member of the *tbx1* subfamily, which consists of *tbx1*, 10, 15, 18, 20, 22 [9]. *tbx1* has been shown to regulate oral epithelial adhesion and palatal development [15] and the *van gogh/tbx1* zebrafish mutant results in severe craniofacial defects similar to the complex defects found in DiGeorge syndrome [16]. Mutations in the human *tbx22* gene cause syndromic, X-linked cleft pa-

late/ankyloglossia and also strongly contribute to non-syndromic cleft lip and/or cleft palate and cleft palate alone [13,17-21]. Therefore, we asked whether or not zebrafish *tbx22* plays a similar role in palate formation and what role it plays in craniofacial development.

Characterization of zebrafish *tbx22* revealed two splice isoforms, *tbx22-1* and *tbx22-2* [13]. *Tbx22-1* encodes a protein of 444 amino acids and resembles canonical *Tbx22* orthologs, while *tbx22-2* encodes a 400 amino acid protein that lacks conserved N-terminal sequences [13]. Experiments examining a combined profile of both isoforms revealed that zebrafish *tbx22* is expressed as early as 6 hours post fertilization (hpf) as a low level transcript, and maintains a low level of expression into adulthood [13]. Discrete expression domains are first visible in the pharyngeal mesenchyme and segmental paraxial mesoderm tissue at 28 hpf and are no longer visible at 30 hpf. By 38 hpf a second discrete domain of *tbx22* expression is also found in the perioral mesenchyme underlying the early mouth and in early presumptive jaw joints [13]; however, the function of *tbx22* is still unknown. Zebrafish *tbx22* expression overlaps with expression of *bapx1*, a homeobox transcription factor known to be essential for jaw joint formation [22]. The expression pattern of *tbx22* in zebrafish positions it to be involved in jaw and/or pharyngeal arch development.

Here we focus on the role of *tbx22-2* in the formation of the orofacial complex. We show that knockdown of *tbx22-2* results in mild clefting, ventrally restricted craniofacial cartilages and specific joint defects. Our analysis indicates that the early expression domain of *tbx22-2* is a positive regulator of *osr1*. Early in arch development, decreased *osr1* expression causes endodermal patterning changes that alter the domains of key dorsal/ventral arch signals such as *edn1* and *bapx1* in later development. Furthermore, loss of *tbx22-2* expression may be impacting *gdf5* through decreased *osr1* expression. This work provides insight into the role of *tbx22* in craniofacial development and indicates that *tbx22-2* influences early ventral mesenchyme signals causing dorsoventral defects in positioning of arch elements. The loss of *tbx22-2* also results in joint defects due to altered joint domain expression of *bapx1* and decreased *gdf5* expression.

2. MATERIALS AND METHODS

2.1. Morpholino Injections

Morpholinos were created by Gene Tools Inc. (Philomath, OR), based on the sequences of *tbx22-1* and *tbx22-2*. The *tbx22-2* translation blocking morpholino is 5'-GGAAATGCAGAGTTCAATGTAAACG-3'.

The translation blocking mismatch (*tbx22-2*-MM) morpholino is 5'-CACGAGTGTAAACTTTCGTCATAG-3'.

The splice blocking morpholino sequences are as follows: *Tbx22* exon5-MO

5'-TCCATGAATTGGCAAGTTACCTGTT-3'; *tbx22* exon4-MO 5'-TACTGAAAAAGGGCACTCACATGGC-3'. The *tbx22*-exon-MM morpholino 5'-TTTCAAATGTCTCTCCACTCTACCT-3'. Each morpholino was prepared at a concentration of 1.0mM. Various dilutions, 1:5 (6.7 ng), 1:7 (5.3 ng), 1:10 (3.0 ng) were used to inject approximately 1.5 nl into 1 - 4 cell stage embryos to determine a concentration that produced moderately severe phenotypes. Morpholinos were injected using a pico-injector PLI-100. The 1:5 dilution produced a moderately severe phenotype and was used for all remaining experiments. Missense morpholinos were also injected to confirm that any developmental defects were the result of *tbx22* knockdown and not a side effect of physical injection. Missense morpholinos produced no phenotype and are referred to as "wild-type" in figures. The embryos were monitored daily and collected at various stages of development for study.

Morpholino rescues were performed using synthetic capped mRNA synthesized from full length *tbx22-1/2* clones using the Ambion Mmessage machine kit (Ambion, Austin Tx). Approximately 1 - 4 nl of a 250 ng/ul solution was injected into 1 - 4 cell stage embryos. An equal mixture of *tbx22-1* and *tbx22-2* mRNA was used for rescue of the splice blocking morpholinos.

2.2. Alcian Blue Cartilage Staining

Alcian Blue Staining was used to visualize cartilages in larvae [23]. Six day old missense MO injected (wild type), *tbx22-2*-MO and *tbx22* exon-MO injected larvae were euthanized in tricaine and fixed in 4% paraformaldehyde overnight. Larvae were washed with PBS-Tween (PBT) to remove paraformaldehyde, bleached in 30% hydrogen peroxide to remove pigment, and then washed in PBT again. Larvae were incubated in 0.3 mg/ml alcian green/acetic acid for 4 hours, rehydrated in a staged ethanol series and treated with 25 mg/ml trypsin to dissolve brain tissue and allow visualization of pharyngeal arch cartilages. Larvae were observed in 75% glycerol. Morpholino injected larvae were catalogued for presence/absence and defects in each craniofacial element compared with wild type larvae. Craniofacial cartilages of wild type (5 larvae) and *tbx22* exon4-MO (15 larvae) embryos were dissected out of the larvae in glycerol and were flat mounted on glass slides. Bright-field images were taken of each individual cartilage element using the Olympus 12.5 megapixels color digital camera.

2.3. RNA Extraction and Quantitative RT-PCR

Developmentally staged zebrafish were collected homogenized in trizol and stored at -80°C. Total RNA was

isolated using Trizol according to manufacturer's instructions (Invitrogen, Carlsbad, CA), and 4.5 µg of each total RNA sample was used in RT reactions using the SuperScript III First-Strand Synthesis System for RT-PCR (Invitrogen, Carlsbad, CA). The resulting RT products (1 µl) were used as template in 50-µl PCR reactions, performed with Platinum PCR SuperMix High Fidelity (Invitrogen, Carlsbad, CA), using the following reaction conditions: denaturation at 95°C for 5 minutes followed by 35 cycles of 95°C for 40 seconds, 60°C for 1 minute, and 72°C for 2 minutes, followed by a final extension at 72°C for 7 minutes. Negative control is total RNA with no reverse transcriptase added in cDNA reaction. Internal primers were designed to span introns to ensure that no gDNA contamination occurred.

Quantitative-PCR—Real-Time PCR was performed with SYBR-Green chemistry, using a Roche Lightcycler. β -actin served as an internal reference. The following primers were designed for quantitative RT-PCR: β -actin Q For 5'-CTTCTTGGGTATGGAATCTTGC-3', rev 5'-GTACCACCAGACAATACAGTG-3', *tbx22a*Q For 5'-CACGCGACAAGTGGATCATA-3', rev-5'-CTCAGATCCTGTGCGTCAAA -3', *tbx22-2*Q For 5'-CACGCGACAAGTGGATCATA-3', rev 5'- CACTAACCCTGTGCGTCAAA -3'; *mef2ca* Q for-5'- CGCACGAGAGTCGGACTAAT-3', *mef2ca* Q rev-5'- GGTCGATGTCTCGTTGATT-3', *edn1*Q for 5'-CTGGAATACGGACTTGCAT-3', *edn1* Q rev 5'-TGTCCAGGTGGCAAAAGTAG-3'; *gdf5* Q for 5'-AGCCTTCTTCGTGGTGTGTTG-3', *gdf5* Q rev 5'-GCATCTCTGTTTGGGGTTCT-3'; *hand2* Q for 5'-CAGACGCCAAAGAAGAAAGG- 3', *hand2* Q rev 5'-GTTTCAGATGGCCTCATTTCG -3'; *osr1* Q for 5'-CATGCTGAGGAAGACGAACA -3', *osr1* Q rev 5'-AAGAAGGGTGAAGAGGCACA- 3'; *chd1* Q for 5'-GGTCTGATGCACTGCGTTAT-3', *chd1* Q rev 5'-CATGATTTGCAGCAGTGTCC-3'. For the time course experiment an arbitrary value of 1 was assigned to the average expression at the 1 hpf cell stage and expression level at other time points was normalized to this denominator. For analysis of various genes in MO-injected embryos the Wt sample was assigned a value of 1 and expression level at other time points was normalized to this denominator. Plots of quantitative RT-PCR are the average 3 individual biological replicates.

2.4. Whole Mount *in Situ* Hybridizations

Bacterial cultures (*bapx1*, *dlx2a*, *edn1*, *nkx2.3*, *sox9a*) were inoculated with transformed cells and incubated overnight at 37°C. Plasmids were isolated using QIaprep miniprep protocol (Qiagen, Valencia, CA). Plasmids were linearized as follows: *bapx1*/BamHI, *dlx2a*/BamHI, *edn1*/EcoRI; *foxa2l*/SacI, *nkx2.3*/HindIII. The restriction

digest was cleaned using equal volume phenol: chloroform extraction and Manual Phase Lock Gel (5-Prime, Gaithersburg, MD) columns. The linear template was precipitated with 1/10 the volume 3 M sodium acetate and 3 times the volume of 95 percent ethanol. Riboprobe templates for *hand2* and *osr1* were synthesized by PCR using platinum PCR supermix. PCR conditions were as follows: 94°, 5 minutes, 94°, 40 seconds, 60°, 30 seconds, 72°, 1 minute, 72°, 5 minutes, 35 cycles. Primer sequences: *osr1* forward 5'-TGGATAACCGTATTACCGCC-3' *osr1* reverse

5'-CGCGCAATTAACCCTCACTAAAGCACTAGTCA TACCAGGATC-3' *hand2* forward 5'-TGGATAACCGTATTACCGCC-3', *hand2* reverse 5'CGCGCAATTAACCCTCACTAAAGCACTAGTCA TACCAGGATC-3'. (Underline indicates T3 polymerase binding site). The PCR product was purified using the Montage PCR centrifugal filter device protocol (Millipore, Woburn, MA).

Riboprobes were synthesized using the DIG RNA Labeling Kit (T3/T7) (Roche Applied Science, Indianapolis, IN). WISH was performed as previously described [24], using a modification of published protocols [25]. Embryos were cleared in glycerol and photographed. All images were captured on an Olympus SZX12 microscope and assembled using Adobe Photoshop.

3. RESULTS AND DISCUSSION

3.1. Differential Expression of the *tbx22-1* and *tbx22-2* Transcripts throughout Larval Development

Initial analysis of the *tbx22-1* and *tbx22-2* transcripts using standard reverse transcriptase PCR (RT-PCR) revealed expression of both transcripts consistently throughout adulthood [13]. The initial studies indicated that *tbx22-1* was the only maternal transcript, and the other stages examined revealed relatively equal levels of transcription of both isoforms using end-point PCR [13]. Since the *tbx22-2* transcript is a mere 113 bp larger than the *tbx22-1* transcript, assaying for differential expression of the two transcripts was not successful using whole mount *in situ* hybridization. We used quantitative PCR (Q-PCR) to determine if there was any difference in expression between the two transcripts. Q-PCR is more sensitive than standard RT-PCR, often revealing differences in expression not resolved by standard gel electrophoresis. Q-PCR revealed that *tbx22-2* expression is higher than *tbx22-1* as early as 11 somites (som). *Tbx22-2* continues to be the dominant transcript from 11som through 28 hpf (**Figure 1**). The two transcripts become more equally expressed by 38 hpf. This time period is interesting as it is prior to the discrete expression in the stomodeum region we see by 38 hpf. By the 10 somite

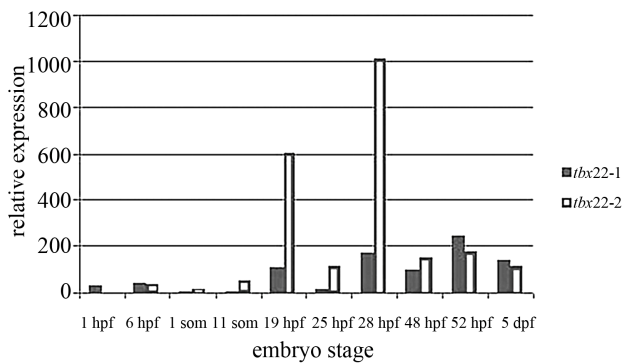


Figure 1. Developmental Q-PCR profile of *tbx22-1/2* mRNAs. Quantitative PCR reveals dramatic increases in *tbx22-2* transcript over *tbx22-1* transcripts between 11 somite stage and 28 hours post fertilization (hpf). Q-PCR analysis reveals that at 19 hpf and 28 hpf *tbx22-2* is expressed nearly 5× greater than *tbx22-1*.

stage neural crest cells begin to migrate from the dorsal neural keel, and are positioned in pharyngeal pouches by 28 hpf. As noted, the only other visible expression domain of *tbx22* was the ventral pharyngeal mesenchyme and segmental paraxial mesoderm at 28 hpf [13], we will refer to this expression as the early *tbx22-2* expression domain, while the bilateral expression after 38 hpf is the late expression domain.

While early *tbx22* expression is likely to impact various tissues, our interest lies specifically in mouth formation. We next examined *tbx22* expression in head vs. tail tissue. Reverse transcriptase PCR revealed that at 48 hpf the dominant transcript is *tbx22-2* in both the head and tail, with minimal *tbx22-1* expression in the head at this time (Figure 2). These results in conjunction with the peaks in expression led us to focus in on the role of *tbx22-2* in development of the craniofacial region.

3.2. *tbx22* Knockdown Results in Defects in Positioning of Pharyngeal Arches 1 and 2 Ventral Elements and Defects in Pharyngeal Arch Joint Formation

A morpholino (MO)-mediated gene knockdown strategy was used to examine the role of *tbx22-2* on craniofacial cartilage development. Wild type (mismatch MO injected), *tbx22-2*-MO and splice blocking MO injected embryos were stained at 6 dpf with alcian blue, which stains acid glycosaminoglycans present in cartilage [25]. Each injected larvae was analyzed for the presence/absence of individual pharyngeal cartilage elements as well as any deviations from normal patterning when compared with normal embryos.

Tbx22-2-MO and *tbx22* exon4/5-MO larvae displayed nearly identical phenotypes with clear defects in the ventral positioning of the first and second branchial arches, and incompletely fused trabeculae with a more severe

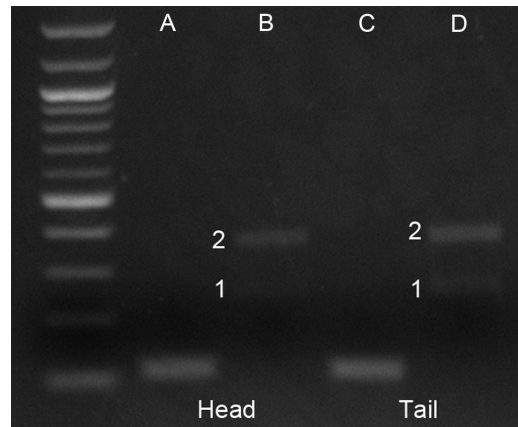


Figure 2. Analysis of Head and Tail expression of *tbx22-1/2* mRNAs. Reverse Transcriptase PCR was used to examine transcript levels in severed heads and tails at 48 hpf. Head cDNA (A, B), and Tail cDNA (C, D). *Tbx22-1* and *tbx22-2* fragments are labeled 1 and 2 respectively (B,D). Beta-actin was used as a control (A,C). Results show that *tbx22-2* is the predominant transcript in the head, while the tail has a higher level of *tbx22-1* expression than the head but *tbx22-2* is still the more abundant transcript.

defect in the *tbx22* exon4/5-MO larvae (indicated by Figure 3). Translation blocking morpholinos target the ATG start site specifically of *tbx22-2*. We also used splice blocking morpholino's to confirm that loss of *tbx22* was causing the observed phenotype. Splice blocking morpholinos target an intron-exon boundary which causes an altered gene product vs preventing translation. This splice blocking approach can utilize RT-PCR to assay altered mRNA and hence overall decrease in functional protein. In our case, the splice blocking morpholino also blocks both isoforms of *tbx22* making it a more severe defect. All *tbx22-2*-MO fish (n = 55) possessed the Meckel's cartilage; however 54% of larvae had a ventrally restricted Meckel's (Figures 3(B) and (B')). After examining the dissected Meckel's cartilage, it was clear that *tbx22-2*-MO injected larvae exhibited defects in the retroarticular process of the Meckel's cartilage (Figures 4(a), Panel D). The ceratohyal cartilage was present in all *tbx22-2*-MO injected larvae but was ventrally restricted in 67% of larvae (Figures 3(B) and (B')). The patterning defects in the Meckel's cartilage and the ceratohyal cartilage were the most common defects seen in lower jaw elements in the injected larvae. Both the Meckel's and ceratohyal cartilages develop from ventral condensations of cranial neural crest cells, suggesting that *tbx22-2* plays a role in patterning ventral cartilages. The dorsal arch elements, palatoquadrate and hyosymplectic cartilages were smaller but normally positioned. However, *tbx22-2*-MO injected larvae had visible breaks in the hyosymplectic cartilage (53%) which corresponded to a noticeable loss of the interhyal, second arch joint

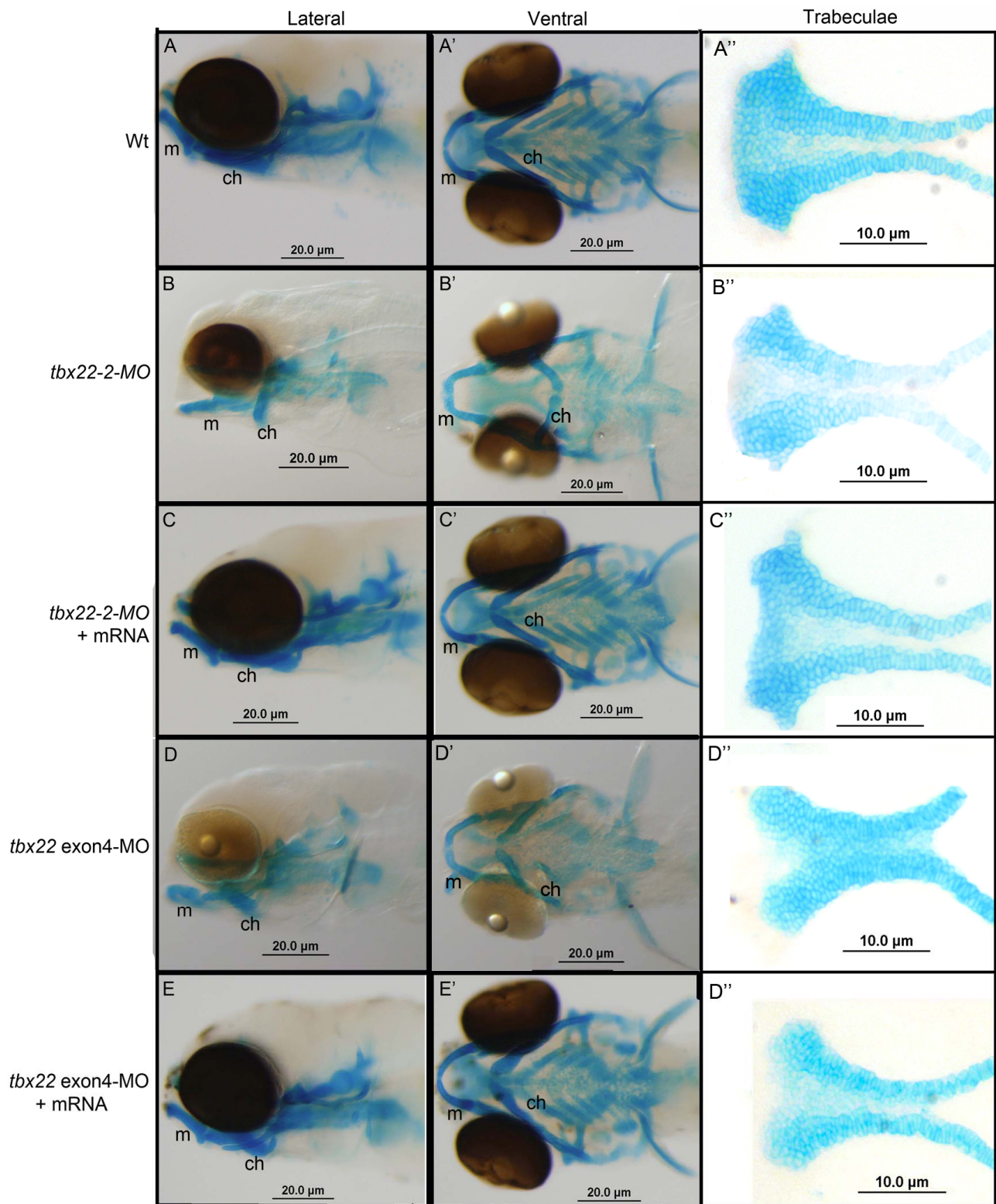


Figure 3. Cartilage phenotypes of *tbx22* knockdown embryos. Alcian Blue cartilages staining of 6 dpf wild type, *tbx22-2-MO*, *tbx22exon4-MO* and *tbx22exon5-MO* larvae. A, A') lateral and ventral views of mis-sense control (wt) larvae. B, B') *tbx22-2-MO* injected embryo. C, C') *tbx22-2* mRNA rescued larvae D, D') *tbx22exon4-MO* injected embryo E, E') *tbx22-1/2* mRNA rescued *tbx22exon4-MO* larvae—both the Meckel's cartilage and the ceratohyal are ventrally restricted and smaller than wild type larvae. Dissected trabeculae from each embryo represented with area of cleft indicated by red asterisk. Abbreviations: Ch-ceratohyal, M-Meckel's.

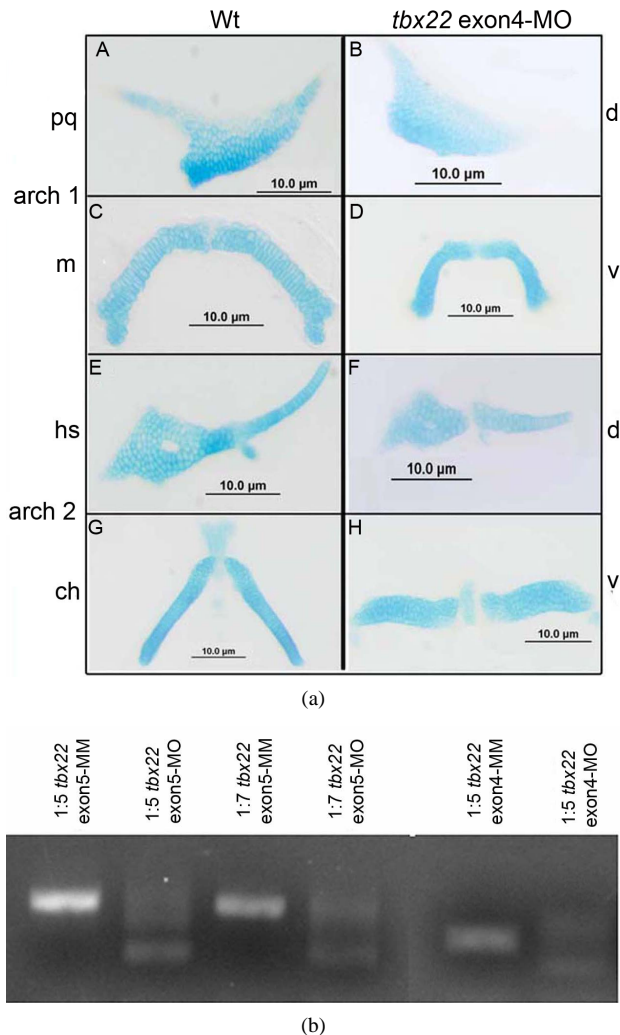


Figure 4. Dissected *tbx22* knockdown cartilages. (a) Dissected and flat-mounted cartilage elements from wild type (A, C, E, G), *tbx22*exon4-MO injected (B, D, F, H) 6 dpf larvae. Arch 1 (mandibular) dorsal (d) and ventral (v) components are the palatoquadrate (pq) and the Meckel's (m), respectively. Arch 2 (hyoid) arch dorsal and ventral components are the hyosymplectic (h) and the ceratohyal (ch), respectively. (b) Reverse Transcriptase (RT) PCR analysis of altered splicing of exon5 or exon4 upon morpholino injection. Loss of exon 5 results in a product 168 bp smaller, while loss of exon 4 results in a loss of 175 bp.

region, which articulates at the location of the break (**Figures 4(a)**, panel **F**). Each defect was rescued by injection of *tbx22-2* mRNA (**Figures 3(C)** and **(C')**).

Splice blocking morpholinos (*tbx22* exon4-Mo, *tbx22* exon5-MO) were designed to test the specificity of the effect of the translation blocking morpholino. The Meckel's cartilage was ventrally restricted in 79% - 81% (**Table 1**) of the splice blocking-MO injected larvae (**Figures 3(D)** and **(D')**) and this was accompanied by defects in the joint region of the Meckel's cartilage (**Table 1**) similar to the defects seen in the *tbx22-2*-MO injected larvae. Similarly, the ceratohyal elements were ventrally restricted in 82%

- 85% of the splice blocking-MO injected larvae (**Table 1**). The palatoquadrate cartilage was smaller than controls but normally shaped, and the hyosymplectic possessed similar defects and loss of the second arch joint in 69% - 75% of cases (**Table 1**).

Loss of *tbx22* signals consistently results in clefting of the zebrafish palatal element, the trabeculae. Similar to the other elements, the splice-blocking morpholino causes a more severe cleft than the *tbx22-2*-MO. Analysis of cDNA from splice blocking-MO injected embryos reveals a dose dependent decrease in wild type splicing which correlated with the observed phenotype (**Figure 4(b)**). The highest concentration of morpholino injected (6.7 ng) revealed consistent patterning defects and higher concentration of morpholino, both splice blocking and *tbx22-2*-MO, resulted in severe developmental defects that prevented analysis of craniofacial cartilages. While the overall patterning defects were the same with each morpholino tested, there was a higher percent of defects in the splice blocking-MO injected embryos. This is likely due to the fact that any splice blocking morpholino will cause defects in both *tbx22-1* and *tbx22-2* transcripts since these only differ by a small region.

3.3. Gene Expression Analysis

Previous studies revealed two discrete expression domains for *tbx22* [13]. While *tbx22* is expressed as early as 6 hpf, the first domain of expression is visible in the ventral pharyngeal mesenchyme by 28 hpf. A later domain of expression is found from 38 hpf through 60 hpf as discrete, bilateral domains at either corner of the forming mouth. This later oral ectoderm domain has overlapping expression with *bapx1* [13].

To determine the role of the early *tbx22-2* expression, we examined the patterning of the pharyngeal arches as well as pharyngeal endoderm in the *tbx22*-MO injected larvae. By 28 hpf the pharyngeal pouch system is well developed with NCC's streaming into endodermal pouches which lay the foundation for cartilage differentiation. We asked if *tbx22* expression was required for patterning of the pharyngeal pouches. Analysis of the NCC's as well as the endoderm lining the pouches reveals mis-patterned pouches that do not appear to be normally angled towards the anterior of the embryo. Instead, they appear to migrate more ventrally. This ventral position can be seen in the pattern of streaming NCC's, *dlx2a* expression (**Figure 5(A')**), as well as in the positioning of the endoderm, *nkx2.3* staining (**Figure 5(C')**). The pouch structure is perturbed as early as 24 hpf as indicated in the *sox10:eGFP* line (**Figure 5(B')**). Levels of *foxa2* expression do not seem dramatically affected by *tbx22* knockdown, however, there is a patterning defect in the endoderm. *Tbx22* morphants have a narrowed pharyngeal endoderm but *foxa2* expression is normal (**Figure 5(D')**).

Table 1. Effect of *tbx22* knockdown by translation-blocking and splice-blocking morpholinos on ventral position of meckels and ceratohyal cartilages, and defects in the first and second arch joint elements.

Morpholino	Ventrally restricted		Ventrally restricted		Hyosymplectic		Total #
	Meckels	1st arch joint defect	Ceratohyal	2nd arch joint defect	defect	of injected embryos	
<i>tbx22-2-MM</i>	0	0	0	0	0	60	
<i>tbx22-2-MO</i>	54%	65%	67%	50%	48%	55	
<i>tbx22</i> exon MM	0	0	0	0	0	75	
<i>tbx22</i> exon4-MO	81%	78%	82%	77%	69%	72	
<i>tbx22</i> exon 5-MO	79%	81.50%	85%	75.50%	74.50%	77	

Pharyngeal arch cartilage phenotypes seen in 6 dpf larvae for all three morpholino's examined. *Tbx22-2-MO* is an AUG translation blocking morpholino while the others are exon4 or 5 splice blocking morpholinos. Each percent represents a defect in both elements, there was a few larvae that only one element was seen resulting in a portion of a % in some cases. This partial percent does not represent asymmetry in effect.

Surprisingly, *osr1*, which is also expressed in the endoderm, anterior ventral mesenchyme (avm) as well as in the branchial arches (**Figure 5(E')**) is severely reduced in the *tbx22* morphants. *Osr1* is a gene that belongs to the odd-skipped gene family, and has been shown to be expressed in the mouse intermediate mesoderm, branchial arches, and ventral mesenchyme [27,28]. In zebrafish *osr1* is expressed robustly in the ventral head mesenchyme and branchial arches but its role in craniofacial development has not been examined. *Osr1* has been shown to be essential for kidney formation [29], and recently has been shown to interact with *tbx5a* during pectoral fin development [30]. Here we show that *osr1* is severely disrupted by loss of *tbx22-2* expression. Quantitative PCR analysis revealed a 60% - 70% decrease in *Osr1* expression between 36 - 48 hpf (**Figures 7(c)** and **(d)**).

The second, later expression domain of *tbx22*, in the developing mouth region overlaps with *bapx1* [13]. *Bapx1* is a member of the endothelin (*edn1*) signaling pathway and is involved in joint formation [22]; furthermore, all *tbx22-MO* injected embryos have ventral positioning defects. Since the *edn1* pathway is the major ventral specification pathway, we examined the effect of shape of the developing pharyngeal pouches.

Edn signaling is a tightly regulated pathway that has many intermediates. *Tbx22* is a mesodermally expressed transcription factor and is likely to be exerting its effect on molecules within the mesoderm. Alterations in mesodermal patterning could cause arch positioning defects, so we next asked what molecules influence *edn1* levels that are positioned well to be influenced by *tbx22*. *Mef2ca* is a transcription factor that plays a critical role in mesoderm development and has been shown to be required to effect *edn1* signaling in the cranial neural crest [31]. Loss of *mef2ca* signaling results in less severe craniofacial defects than *edn1* mutants, however, loss of *mef2ca* has striking similarities to the phenotype observed in *tbx22* knockdowns [31]. Analysis of spatial expression

patterns of several major *edn1* pathway components by whole mount *in situ* analysis reveals slight patterning changes in *tbx22-MO* knockdowns. The *bapx1* expression domain in *tbx22-2-MO* injected embryos reveals a posterior shift and cells that are positioned more laterally (**Figures 6(A)** and **(B)**), similar to changes the endothelin expression domains (**Figure 6(D)**, asterisks). The cluster of *bapx1* expressing cells also appears to be more ventrally positioned. *Bapx1* is downstream of *edn1* and examination of *edn1* in *tbx22* morphants reveals a gap in the *edn1* expression domain (**Figure 6(D)** asterisks). The *edn1* domain appears narrowed in the A-P plane but extended laterally (**Figure 6(D)**, open arrow) mirroring the narrowed ventrally restricted *bapx1* expression domain. *Hand2* expression levels and patterning appear unaffected by *tbx22-2* knockdown (**Figures 6(E)** and **(F)**). The observed changes in ventral positioning of these cell populations may result from changes in patterning of the pharyngeal endoderm and shape of the developing pharyngeal pouches.

Alterations in mesodermal patterning could cause arch positioning defects, so we next asked what molecules influence *edn1* levels that are positioned well to be influenced by *tbx22*. *Mef2ca* is a transcription factor that plays a critical role in mesoderm development and has been shown to be required to effect *edn1* signaling in the cranial neural crest [31].

Loss of *mef2ca* signaling results in less severe craniofacial defects than *edn1* mutants, however, loss of *mef2ca* has striking similarities to the phenotype observed in *tbx22* knockdowns [31]. *Mef2ca* mutants have open mouths, ventrally restricted jaws and joint loss [31], similar to the defects we see in *tbx22-2* knockdown embryos. We assayed the level of expression of *mef2ca* as well as several *edn1/bapx1* related genes. Previous work had demonstrated that *edn1* signaling is required for *bapx1* and *hand2* expression [22]. Gene clusters can be grouped by those with direct interaction with *edn1* or genes that act downstream of *edn1*. We examined two

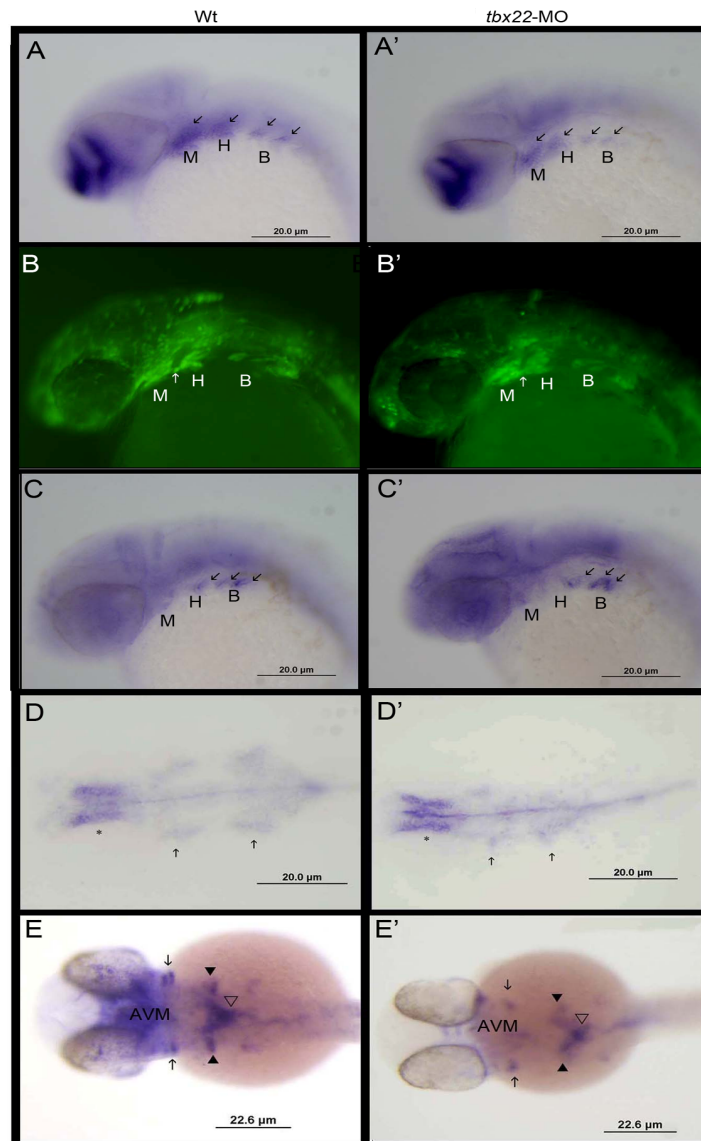


Figure 5. Analysis of pharyngeal arch/pouch patterning in *tbx22* knockdowns. Lateral views of *dlx2a* expression in 32 hpf wild type (A) and *tbx22*exon4-MO (A') injected embryos. *dlx2a* is expressed in neural crest cells in the pharyngeal pouches as well as the diencephalon of the brain. Fluorescent *sox10* expression in 24 hpf wild type (B) and *tbx22*exon4-MO (B') injected zebrafish embryos. *Sox10* is expressed in neural crest cells in 24 hpf embryos. By 24 hpf cranial neural crest cells have migrated into the pharyngeal arches. As with the *dlx2a* staining the arches seem more ventrally oriented compared to the anterior streaming position of the normal arches. *Nkx2.3* is expressed in the endodermal cells of the pouches at 35 hpf in wild type (C) and *tbx22*exon4-MO (C') injected embryos. Specifically, the domain between the Meckels (M) and Hyoid (H) arch (white arrow, C-C') is oriented more ventrally compared the pouch in the normal embryos. Similar ventral restriction is observed. Overall endoderm patterning was examined using *foxa2* at 28 hpf. *Foxa2* is expressed in the pharyngeal endoderm (arrows) and appears normal in *tbx22* morphants (D') compared to wild type (D), although the endoderm is mediolaterally narrowed in the *tbx22* morphants. At 32 hpf *osr1* expression (E,E') in the anterior ventral mesenchyme (avm) is severely reduced as well as in the anterior branchial arches (arrows), but appears normal in the more posterior ceratobranchial arches (black arrow heads).

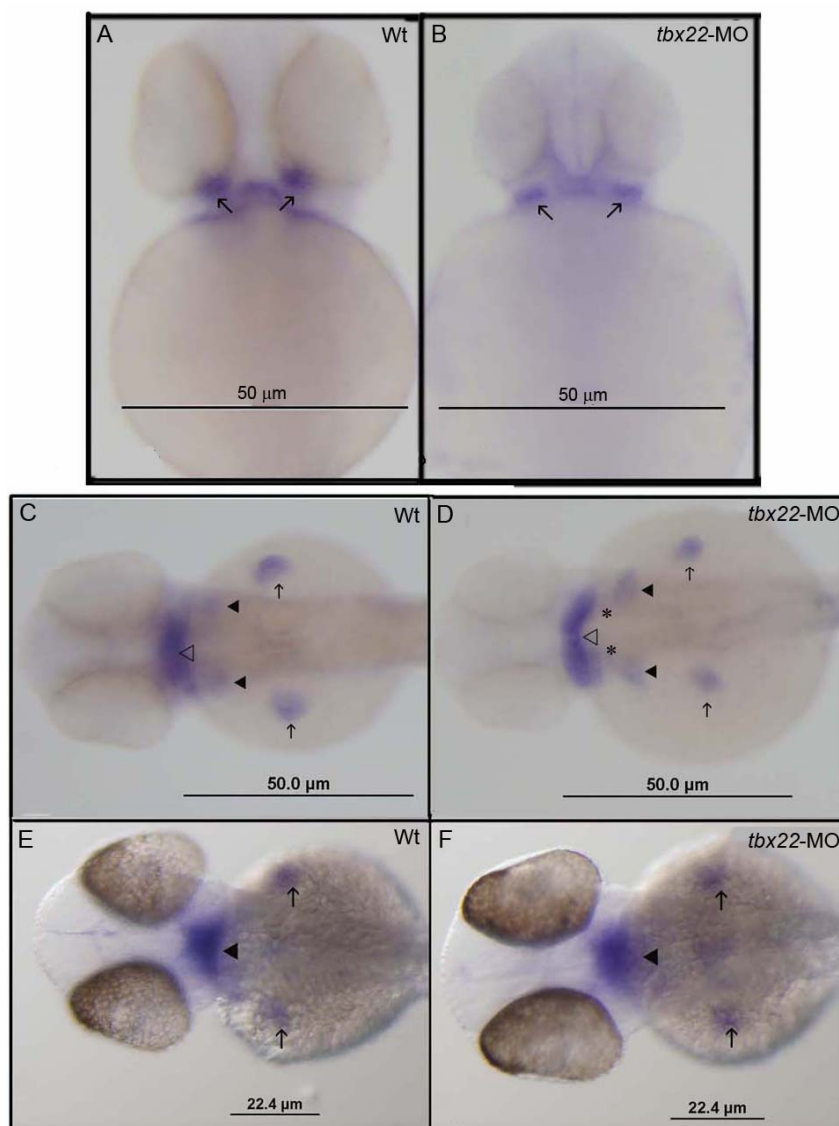


Figure 6. Spatial expression defects in *edn* signals in *tbx22* knockdown embryos. *Bapx1* expression in 50 hpf wild type embryos (A) and *tbx22*-2-MO injected embryos (B). *tbx22*-2-MO injected embryos appear to exhibit an altered domain of *bapx1* expression in the intermediate joint region compared with wild type embryos. Arrows indicate *bapx1* expression in the early jaw joint. Ventral view of *edn1* expression in 48 hpf zebrafish in wild type (C) and *tbx22*-2-MO injected (D) embryos. *Edn1* is expressed in the pharyngeal arches, heart and mesoderm (open arrowhead), the early ceratobranchial arches (arrowheads) and the pectoral fins (arrows). The *edn1* expression domain appears to be laterally extended in *tbx22*-2-MO injected embryos, especially in the anterior mesoderm (open arrowhead). Ventral views of *hand2* expression at 48 hpf in wild type embryos (E) and *tbx22*-2-MO embryos (F). *Hand2* expression in the pharyngeal arches (arrowheads) and in the pectoral fins (arrows) does not appear to be affected.

time points to assay early arch events and later arch events, 29 hpf and 48 hpf respectively (**Figures 7(a) and (b)**). At 29 hpf early *mef2ca* expression is decreased in *tbx22*-MO injected embryos and no significant change in *edn1* or *hand2* is observed (**Figures 7(a) and (b)**). By 48 hpf *mef2ca* levels appear to return to a more normal level

of expression, and this is confirmed with quantitative PCR analysis at 50 hpf (**Figure 7(a)**). Since *tbx22* has a very discrete bilateral expression domain surrounding the mouth, we also asked whether or not there is a local effect on *bapx1* or its signaling partners. Endpoint RT-PCR revealed a decrease in *gdf5* but not *chd* at 50 hpf

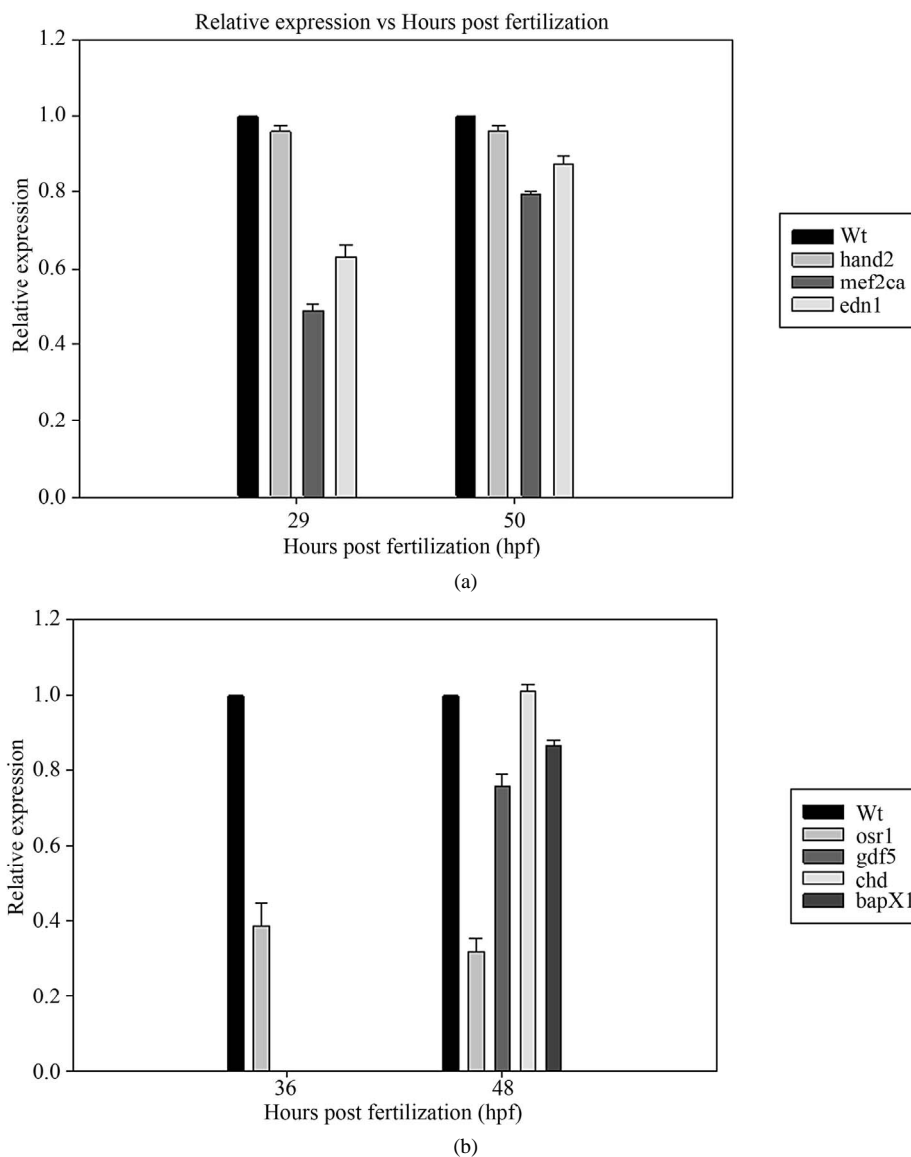


Figure 7. Analysis of endothelin signals in *tbx22* knockdowns. Quantitative Reverse Transcriptase PCR (RT-PCR) analysis of various *endothelin* signaling partners in *tbx22*exon4-MO injected embryos. (a) RT-PCR analysis of *mef2ca*, *edn1*, *hand2* with the *b-actin* control for relative expression level. Results reveal a significant ($p < 0.001$) decrease in *mef2ca* expression at 29 hpf and 50 hpf; (b) RT-PCR analysis of chordin (*chd*), *gdf5*, *bapx1*, *osr1* at 50 hpf reveals a significant ($p < 0.001$) decrease in *osr1* at both 36 and 48 hpf, and *gdf5* and *bapx1* at 48 hpf. Expression was normalized to *beta-actin* in each sample which represented 1 \times expression level and *tbx22* MO knockdowns are presented as a percentage of normal expression.

(**Figure 7(b)**), Q-PCR analysis of *bapx1* and its signaling partners *gdf5* and *chd* reveal a 15% decrease in *bapx1* expression and a 25% decrease in *gdf5* expression in *tbx22* morphants (**Figure 7(b)**).

4. CONCLUSIONS

In the present study we have examined the role of zebrafish *tbx22* in craniofacial development. This work has demonstrated that loss of *tbx22* signals causes ventral

arch positioning defects as well as first and second arch joint defects, and a mild clefting of the zebrafish palatal element. This palatal clefting is similar to mammalian cleft palate which has been linked to defects in *Tbx22* signals. These preliminary studies suggest that the zebrafish will be a useful model to investigate the role of *tbx22* in palate development. Dissecting the requirement of any gene during development must take into consideration the timing of knockdown and whether or not defects are due to developmental delays or specific expres-

sion of key signals. For this reason we have described what we believe to be the role of early *tbx22-2* expression in the developing zebrafish embryo. The first discrete *tbx22* expression domain is the ventral pharyngeal mesenchyme and somitic mesoderm. We have shown that loss of *tbx22-2* signals at this early time, 28 hpf, resulted in defects in the shape of the developing endodermal pouches (**Figure 5**).

This early mis-patterning has consequences, such as mis-positioned arch elements and an overall size reduction in the craniofacial complex of *tbx22*-morphants. We have also revealed another role for zebrafish *osr1* in development. Loss of *tbx22* signals dramatically decreases *osr1* expression as seen in whole mount stains and quantitative PCR.

Osr genes have been well characterized for their involvement in kidney formation, as well as pectoral fin development. Vertebrate *Osr* genes are expressed in many tissues and have been shown to be required for proper formation and/or patterning of the heart, endoderm, teeth, palate, the bones and synovial joints in the limbs [28,32-36]. While no studies have defined the specific requirement of *osr1* in zebrafish craniofacial development, recent work has shown that *osr1* and *tbx5a* interact to drive proper formation of the pectoral fins [30].

The second later domain of *tbx22* expression poses a challenge in regards to analyzing its role in mouth formation. Clearly, the morpholino gene knockdown technique causes a loss in the early expression of *tbx22-2* which impacts overall endodermal patterning preventing analysis of the discrete mouth domains by 38 hpf. However, the later expression of *tbx22* which overlaps with *bapx1* expression positions it well to interact with *endothelin 1* signals.

Edn is known to act as a morphogen affecting two developmental fates, joint formation and ventral cartilage formation [22]. *Edn1* acts through *bapx1* in specifying joint formation while *hand2* is an intermediate for ventral cartilage formation [22]. *Mef2ca*, which is expressed in postmigratory cranial neural crest within pharyngeal arch primordia, has recently been shown to be an effector in the *edn1* pathway [31]. *Mef2ca* function is required for expression of many *edn1*-dependent target genes including *bapx1* [31]. Members of the *MEF2* family have been shown to bind *Tbx* transcription factors, specifically *MEF2C* binds *tbx5* in heart formation [37]. Furthermore, previous work has shown that *tbx1* is required for pharyngeal arch expression of *edn1* [38], and *tbx22* is grouped within the *TBX1* subfamily [39]. Knowing that evidence exists for a substantial role for *tbx*-binding proteins in regulating endothelin signaling, and with zebrafish *tbx22* being expressed with *bapx1*, we examined the effect of *tbx22-2* knockdown on components of the *edn1* pathway.

Analysis of the endothelin-1 signaling pathway reveals that decreased *tbx22* results in decreased expression of *bapx1* and altered expression domains of *bapx1* and *edn-1*. There is, however, no decrease in *hand2* expression. We believe that knockdown of *tbx22-2* causes perturbations in tissue patterning resulting in spatial defects in *edn* signals. These results do not support a direct role for *tbx22* in the *edn* pathway. The decrease in *mef2ca* expression at 28 hpf is likely due to changes in heart expression of *mef2ca* and not a specific change in neural crest expression. Our results reveal that the role of *tbx22* on *mef2ca* expression is timing specific, and this change in *mef2ca* expression may be causing observed edema and heart abnormalities. Analysis of a detailed time series of *tbx22* morphants as well as other *mef2ca* signaling intermediates, *dlx5a*, *dlx6a* and *dlx3b*, will provide more detail into the specific requirements for *tbx22* throughout the early stages of arch formation and joint patterning.

While examining the signals downstream of *bapx1*, we did uncover a decrease in *gdf5* expression in the *tbx22-2* knockdown embryos. This decrease in *gdf5* could be the result of a decrease in *bapx1* expression, but this is not supported by the *chd* expression which is unaltered. It is more likely that the *gdf5* levels are being influenced by another factor independent of *bapx1*. *Osr1* has been shown to be required for maintenance of expression of signaling molecules critical for joint formation, including *Gdf5* [30]. This work has also revealed a significant loss of *osr1* signaling in *tbx22* morphants which positions *osr1* as a candidate for mediating the effect of loss of early *tbx22* signals in craniofacial development. Normal expression of *osr1* positions it well to influence craniofacial development, and *osr1* is expressed in the ventral pharyngeal arch mesenchyme, similar to the pharyngeal mesenchyme expression domain of *tbx22* (**Figure 8**) [13,40]. The zebrafish *osr1* gene does have a putative T-binding domain located -419 bp upstream of the transcriptional start site. We predict that *tbx22* binds and influences *osr1* transcription which in turn impacts patterning of the endoderm and is likely to impact *gdf5* levels and joint formation. Furthermore, conditional *Osr1* knockouts in mice have demonstrated a requirement for *Osr1* in heart formation [33] which overlaps with our observed heart defects and decreased *mef2ca* expression during heart formation stages. Current studies are examining the interaction of *osr1* and *tbx22*.

These studies cannot directly address the function of the later time point of *tbx22* expression in the bilateral domains surrounding the developing mouth. Future studies will require either site specific gene knockdown or generation of a *tbx22* knockout that is rescued through the early stages of development to assay specifically mouth formation. TALEN technology is advancing allowing for the potential to generate a *tbx22* mutant

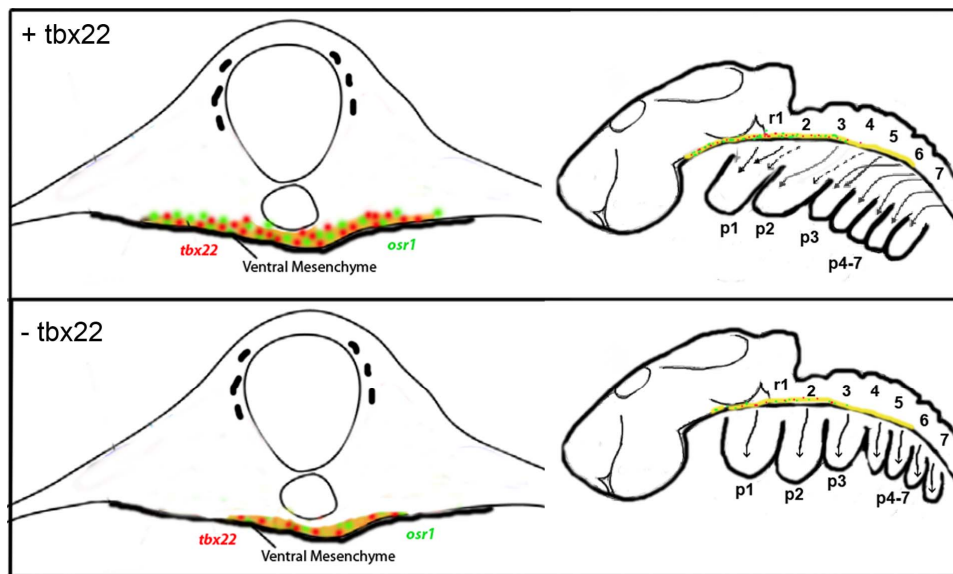


Figure 8. Schematic representation of early *tbx22* expression domain overlap with *osr1*. Both *tbx22* and *osr1* are expressed in the ventral mesenchyme during the early stages of pharyngeal arch formation. Decreased expression of *tbx22-2* (red dots) results in dramatic loss of *osr1* (green dots) in the mesenchyme causing decreased endodermal tissue. The narrowed endoderm results in pharyngeal pouches that do not curve towards the anterior of the embryo (arrows).

[41,42]. However, in regards to the interaction of *osr1* and *tbx22* at this later time point, recently the signals involved in zebrafish palatogenesis have been eloquently displayed by Swartz *et al.*, 2011 [40]. This work reveals neighboring expression domains of *tbx22* and *osr1* surrounding the oral ectoderm at 44 hpf. Therefore, *tbx22*'s influence on *osr1* expression may also be relevant specifically in mouth formation.

Future work is required to determine the difference in function of the *tbx22-1* and *tbx22-2* isoforms. The splice target morpholino's result in similar defects as the *tbx22-2* translation blocking morpholino. *Tbx22-1* may provide some redundant function to compensate for *tbx22-2* loss, which is why the splice morpholino does have a higher % of joint defects and ventral displacement at similar concentrations. However, it is likely that *tbx22-1* may also have another role in development. Efforts are underway to parse out unique expression domains of *tbx22-1* and *tbx22-2*. Promoter analysis may also provide clarity as to the role for two *tbx22* isoforms. Detailed analysis of these regulatory regions will provide much needed clarity into the regulation of *tbx22* signals. Furthermore, promoter analysis may uncover a mouth specific regulatory element that would be helpful in designing experiments to drive mouth specific knockdown of signals that are redundant throughout development, making it very difficult to assay these later developmental events.

5. ACKNOWLEDGEMENTS

We wish to thank, Andrea Moreira and Lane Wilson for their technical

assistance and The Molecular Genetics Core Facility of Children's Hospital Boston. We would also like to thank Dr. Thomas Schilling for sharing the *sox10*: eGFP transgenic line. *This study was carried out in strict accordance with the recommendations in the Guide for the Care and Use of Laboratory Animals of the National Institutes of Health. The protocol was approved by the University of Massachusetts Institutional Animal Care and Use Committee (IACUC), Assurance Number: A4491-01. This research was supported in part by National Institutes of Health (NIH)/National Institute of Dental and Craniofacial Research (NIDCR) grant DE14683 (TLF), and a UMass Dartmouth Healey endowment grant.*

REFERENCES

- [1] Benouaiche, L., Gitton, Y., Vincent, C., Couly, G. and Levi, G. (2008) Sonic hedgehog signaling from foregut endoderm patterns the avian nasal capsule. *Development*, **135**, 2221-2225. doi:10.1242/dev.020123
- [2] Hu, D. and Marcucio, R.S. (2009) A SHH-responsive signaling center in the forebrain regulates craniofacial morphogenesis via the facial ectoderm. *Development*, **136**, 1707-1758. doi:10.1242/dev.026583
- [3] Foppiano, S., Hu, D. and Marcucio, R.S. (2007) Signaling by bone morphogenetic protein directs formation of an ectodermal signaling center that regulates craniofacial development. *Developmental Biology*, **312**, 103-114. doi:10.1016/j.ydbio.2007.09.016
- [4] Alexander, C., Zuniga, E., Blitz, I.L., Wada, N., Le, P., Javidan, P., Zhang, Y., Cho, T., Crump, J.G. and Schilling T.F. (2011) Combinatorial roles for BMPs and Endothelin 1 in patterning the dorsal-ventral axis of the cra-

- niofacial skeleton. *Development*, **138**, 5135-5146. doi:10.1242/dev.067801
- [5] Brown, J.M., Wedden, S.E., Millburn, G.H., Robson, L.G., Hill, R.E., *et al.* (1993) Experimental analysis of the control of expression of the homeobox-gene *Msx-1* in the developing limb and face. *Development*, **119**, 41-48.
- [6] Gibson-Brown, J.J., Agulnik, S.I., Silver, L.M. and Papaioannou, V.E. (1998) Expression of *T-box* genes *tbx2-tbx5* during chick organogenesis. *Mechanisms of Development*, **74**, 165-169. doi:10.1016/S0925-4773(98)00056-2
- [7] Barlow, A.J. Bogardi, J.P. Ladher, R. and Francis-West, P.H. (1999) Expression of chick *Barx-1* and its differential regulation by FGF-8 and BMP signaling in the maxilla primordia. *Developmental Dynamics*, **214**, 291-302. doi:10.1002/(SICI)1097-0177(199904)214:4<291::AID-AJA2>3.0.CO;2-E
- [8] Lan, Y. Liu, H., Ovitt, C.E., Wang, Q., Maltby, K.M. and Jiang, R. (2009) Distinct and synergistic roles of *Osr1* and *Osr2* in craniofacial development. *Developmental Biology*, **331**, 490. doi:10.1016/j.ydbio.2009.05.390
- [9] Papaioannou, V.E. and Silver, L.M. (1998) The *T-box* gene family. *BioEssays*, **20**, 9-19. doi:10.1002/(SICI)1521-1878(199801)20:1<9::AID-BIE S4>3.0.CO;2-Q
- [10] Wardle, F.C. and Papaioannou, V.E. (2008) Teasing out *T-box* targets in early mesoderm. *Genes & Development*, **18**, 418-425.
- [11] Kiefer, J.C. (2004) The *tbx* files: The truth is out there. *Developmental Dynamics*, **231**, 232-236. doi:10.1002/dvdy.20122
- [12] Begemann, G., Gibert, Y., Meyer, A. and Ingham, P.W. (2002) Cloning of zebrafish *T-box* genes *tbx15* and *tbx18* and their expression during embryonic development. *Developmental Dynamics*, **114**, 137-141. doi:10.1016/S0925-4773(02)00040-0
- [13] Jezewski, P.A. Fang, P.K. Payne-Ferreira, T.L. and Yelick, P.C. (2009) Alternative splicing, phylogenetic analysis, and craniofacial expression of zebrafish *tbx22*. *Developmental Dynamics*, **238**, 1605-1612. doi:10.1002/dvdy.21962
- [14] Kochilas, L.K., Potluri, V., Gitler, A., Balasubramanian, K. and Chin, A.J. (2003) Cloning and characterization of zebrafish *tbx1*. *Gene Expression Patterns*, **3**, 645-651.
- [15] Funato, N., Nakamura, M., Richardson, J.A., Srivastava, D. and Yanagisawa, H. (2012) *Tbx1* regulates oral epithelial adhesion and palatal development. *Human Molecular Genetics*, **21**, 2524-2537. doi:10.1093/hmg/dd5071
- [16] Piotrowski, T., Ahn, D., Schilling, T.F., Nair, S., Ruvinsky, I., Geisler, R., Rauch, G., Haffter, P., Zon, L.I., Zhou, Y., Foott, H., Dawid, I.B. and Ho, R.K. (2003) The zebrafish van gogh mutation disrupts *tbx1*, which is involved in the DiGeorge deletion syndrome in humans. *Development*, **130**, 5043-5052. doi:10.1242/dev.00704
- [17] Braybrook, C., Doudney, K., Marcano, A.C.B., Arnason, A., Bjornsson, A., Patton, N.A., *et al.* (2001) The *T-box* transcription factor gene *tbx22* is mutated in X-linked cleft palate and ankyloglossia. *Nature Genetics*, **29**, 179-183. doi:10.1038/ng730
- [18] Haenig, B., Schmidt, C., Kraus, F., Pfordt, M. and Kispert, A. (2002) Cloning and expression analysis of the chick ortholog of *tbx22*, the gene mutated in X-linked cleft palate and ankyloglossia. *Mechanisms of Development*, **117**, 321-325. doi:10.1016/S0925-4773(02)00196-X
- [19] Marcano, A.C.B., Doudney, K., Braybrook, C., Squires, R., Patton, M.A., Lees, M., *et al.* (2004) *TBX22* mutations are a frequent cause of cleft palate. *Journal of Medical Genetics*, **41**, 68-74. doi:10.1136/jmg.2003.010868
- [20] Herr, A., Meunier, D., Muller, I., Rump, A., Fundele, R., Hilger-Ropers, H., *et al.* (2003) Expression of mouse *tbx22* supports its role in palatogenesis and glossogenesis. *Developmental Dynamics*, **226**, 579-586. doi:10.1002/dvdy.10260
- [21] Bush, J.O., Lan, Y., Maltby, K.M. and Jiang, R. (2002) Isolation and developmental expression analysis of *tbx22*, the mouse homolog of the human X-linked cleft palate gene. *Developmental Dynamics*, **225**, 322-326. doi:10.1002/dvdy.10154
- [22] Miller, C.T., Yelon, D., Stainer, D.Y.R. and Kimmel, C.B. (2003) Two endothelin 1 effectors, *hand2* and *bapx1*, pattern ventral pharyngeal cartilage and jaw joint. *Development*, **130**, 1353-1365. doi:10.1242/dev.00339
- [23] Whiteman, P. (1973) The quantitative measurement of alcian blue-glycosaminoglycan complexes. *Biochemical Journal*, **131**, 343-350.
- [24] Thisse, C., Thisse, B., Schilling, T.F. and Postlethwait, J.H. (1993) Structure of the zebrafish *snail1* gene and its expression in wild-type spadetail and no tail mutant embryos. *Development*, **119**, 1203-1215.
- [25] Payne-Ferreira, T.L. and Yelick, P.C. (2003) *Alk8* is required for neural crest cell formation and development of pharyngeal arch cartilages. *Developmental Dynamics*, **228**, 683-696. doi:10.1002/dvdy.10417
- [26] Carney, T.J., Dutton, K.A., Greenhill, E., Delfino-Machin, M., Dufourcq, P., Blader, P., *et al.* (2006) A direct role for *Sox10* in specification of neural crest derived sensory neurons. *Development*, **133**, 4619-4630. doi:10.1242/dev.02668
- [27] Chai, Y. and Maxson R.E. Jr. (2006) Recent advances in craniofacial morphogenesis. *Developmental Dynamics*, **235**, 2353-2375. doi:10.1002/dvdy.20833
- [28] Tena, J.J., Neto, A., de la Calle-Mustiennes, E., Bras-Pereira, C., Casares, F. and Gomez-Skarmeta, J.L. (2007) Odd-Skipped genes encode repressors that control kidney development. *Development Biology*, **301**, 518-531. doi:10.1016/j.ydbio.2006.08.063
- [29] Mudumana, S.P., Hentschel, D., Liu, Y., Vasilyev, A. and Drummond, I.A. (2008) Odd skipped related 1 reveals a novel role for endoderm in regulating kidney versus vascular cell fate. *Development*, **135**, 3355-3367. doi:10.1242/dev.022830
- [30] Neto, A., Mercader, N. and Gómez-Skarmeta, J.L. (2012) The *Osr1* and *Osr2* genes act in the pronephric anlage downstream of retinoic acid signaling and upstream of *wnt2b* to maintain pectoral fin development. *Development*, **139**, 301-311. doi:10.1242/dev.074856

- [31] Miller, C.T., Swartz, M.E., Khuu, P.A., Walker, M.B., Eberhart, J.K. and Kimmel, C.B. (2007) *Mef2ca* is required in cranial neural crest to affect Endothelin1 signaling in zebrafish. *Development Biology*, **308**, 144-157. doi:10.1016/j.ydbio.2007.05.018
- [32] Gao, Y., Lan, Y. and Jiang, R. (2011) The zinc finger transcription factors *Osr1* and *Osr2* control synovial joint formation. *Development Biology*, **352**, 83-91. doi:10.1016/j.ydbio.2011.01.018
- [33] Lan, Y., Liu, H., Ovitt, C.E. and Jiang, R. (2011) Generation of *Osr1* conditional mutant mice. *Genesis*, **49**, 419-422. doi:10.1002/dvg.20734
- [34] Kawai, S., Yamauchi, M., Wakisaka, S., Ooshima, T. and Amano, A. (2007). Zinc-finger transcription factor odd-skipped related 2 is one of the regulators in osteoblast proliferation and bone formation. *Journal of Bone and Mineral Research*, **22**, 1362-1372. doi:10.1359/jbmr.070602
- [35] Wang, Q., Lan, Y., Cho, E.S., Maltby, K.M. and Jiang, R. (2005) Odd-skipped related 1 (*Odd1*) is an essential regulator of heart and urogenital development. *Development Biology*, **288**, 582-594. doi:10.1016/j.ydbio.2005.09.024
- [36] Zhang, Z., Lan, Y., Chai, Y. and Jiang, R. (2009). Antagonistic actions of *Msx1* and *Osr2* pattern mammalian teeth into a single row. *Science*, **323**, 1232-1234. doi:10.1126/science.1167418
- [37] Ghosh, T.K., Song, F.F., Packham, E.A., Buxton, S., Robinson, T.E. and Ronksley, J. (2009) Physical interaction between *TBX5* and *MEF2C* is required for early heart development. *Molecular and Cellular Biology*, **29**, 2205-2218. doi:10.1128/MCB.01923-08
- [38] Piotrowski, T., Ahn, D.G., Schilling, T.F., Nair, S., Ruvinsky, I., Gisler, R., *et al.* (2003) The zebrafish van gogh mutation disrupts *tbx1*, which is involved in the Di-George deletion syndrome in human. *Development*, **130**, 5043-5052. doi:10.1242/dev.00704
- [39] Naiche, L.A., Harrelson, Z., Kelly, R.G. and Papaioannou, V.E. (2005) *T-box* genes in vertebrate development. *Annual Review of Genetics*, **39**, 219-239. doi:10.1146/annurev.genet.39.073003.105925
- [40] Swartz, M.E., Sheehan-Rooney, K., Dixon, M.J. and Eberhart, J.K. (2011) Examination of a palatogenic gene program in zebrafish. *Developmental Dynamics*, **240**, 2204-2220. doi:10.1002/dvdy.22713
- [41] Huang, P., Xiao, A., Zhou, M., Zhu, Z., Lin, S. and Zhang, B. (2011) Heritable gene targeting in zebrafish using customized TALENs. *Nature Biotechnology*, **29**, 699-700. doi:10.1038/nbt.1939
- [42] Moore, F.E., Reyon, D., Sander, J.D., Martinez, S.A., Blackburn, J.S., Khayter, C., *et al.* (2012) Improved somatic mutagenesis in zebrafish using transcription activator-like effector nucleases (TALENs). *PLoS One*, **7**, e37877. doi:10.1371/journal.pone.0037877